

FINITE ELEMENT METHOD APPLIED TO THE ANALYSIS OF MEMS AS TEMPERATURE SENSORS

Marcelo A. Savi, savi@mecanica.ufrj.br
José Luis L. Silveira, jluis@mecanica.ufrj.br
Thiago Pereira Chagas, thiago.chagas@poli.ufrj.br
Universidade Federal do Rio de Janeiro
COPPE – Department of Mechanical Engineering
21.941.972 – Rio de Janeiro – RJ, Brazil, P.O. Box 68.503

***Abstract.** Micro-electromechanical systems (MEMS) are related to devices that have been used as sensors and actuators in different applications. The increasing importance of this subject is due to the possibility of producing small mechanical and electromechanical devices providing a better performance of some microscopic applications with low cost when compared to classical devices. In this regard, there are different examples related to informatics, telecommunications, and automobile industry, providing the miniaturization of classical devices and also the development of new devices and tools. Pressure, temperature, vibration and acoustics are some of the variables usually monitored by MEMS sensors. This contribution discusses the application of MEMS as temperature sensors. Micromechanical resonant sensor using a beam as a sensitive element is investigated exploring the temperature dependence of the first resonance frequency. Finite element method is employed in order to evaluate the influence of dissipation in the general measurements.*

***Keywords:** MEMS, sensors, actuators.*

1. INTRODUCTION

Micro-electromechanical systems (MEMS) are related to devices produced in microscopic scales that have been used as sensors and actuators in different applications. Recent technological developments have increased the possibilities of these applications and different actuation and sensing properties as piezoelectric, piezoresistive, electrostatic, thermal, electromagnetic and optical have been used for distinct purposes.

The increasing importance of MEMS is due to the possibility of producing small mechanical and electromechanical devices providing a better performance of some microscopic applications with low cost when compared to classical devices. The miniaturization of electrical circuits is one of the most important aspects related to the expansion of MEMS applications.

The scale reducing requires a proper analysis in order to establish a comprehension of all phenomena involved. The micro scale analysis is associated with an understanding of the scaling properties of the transduction mechanism, the overall design, the materials and the fabrication processes (Judy, 2001). In this regard, the modeling of MEMS implies physical scaling laws that capture fluctuation between micro and macro scales.

Recently, there is a tendency for the smart MEMS concept using smart materials in order to obtain adaptive devices (Dubuc *et al.*, 2004; Namazu *et al.*, 2007). Besides, the nanotechnology has been used to produce nanoelectromechanical systems (NEMS). Therefore, besides Si that is most commonly used as micromachining material, carbon-based materials have received a lot of attention (Wang & Madou, 2005).

This article discusses the application of MEMS as temperature sensors investigating micromechanical resonant sensor using a beam as a sensitive element. Temperature dependence of the first resonance frequency is explored. The analysis of frequency-temperature relation is essential for this kind of system being the objective of numerous articles, however, there are many effects that are not evaluated in literature. Here, finite element method is employed in order to evaluate the influence of dissipation in the general measurements.

2. MEMS – CLASSIFICATION AND FABRICATION

Micro-electromechanical systems (MEMS) can be broadly divided in two main classes: sensors and actuators. Sensors fall in two categories of application: physical and chemical/biological. Physical sensors measure physical quantities such as temperature, pressure, acceleration, while chemical sensors detect chemical and biological quantities including chemical concentrations, pH etc (Liu, 2006).

As many sensing principles are available for a given application, MEMS sensors can also be classified according to the principle used, such as, electrostatics, piezoresistivity, piezoelectricity and thermal resistivity.

Standard microfabrication processes originating from semiconductor technology are used in combination with dedicated micromachining steps to fabricate three-dimensional MEMS structures. The four basic microfabrication techniques are: deposition, patterning, doping and etching. In deposition step, a thin layer, such as an insulating silicon dioxide film, is deposited on a substrate, and then a light-sensitive photoresist layer is deposited on top and patterned

using photolithography. The pattern is then transferred from the photoresist layer to the silicon dioxide layer by an etching process. After removing the remaining photoresist, the next layer is deposited and structured, and so on (Hierlemann *et al.*, 2003). Doping is used to modify the electrical conductivity of semiconducting materials such as silicon or gallium arsenide. In the case of silicon, doping with phosphorous or arsenic yields *n*-type silicon, whereas doping with boron yields *p*-type silicon. Doping is also used to produce piezoresistive silicon resistors (Lin *et al.*, 1999; Gong, 2004, Kaabi *et al.* 2007, Aravamudhan & Bhansali, 2008, Waterfall, 2008).

Micromachining techniques can be categorized into *bulk micromachining*, where the microstructure is formed by machining a relatively thick bulk substrate material, and *surface micromachining*, which is an additive process where features are built up layer by layer on the surface of a substrate.

The bulk micromachining techniques are etching techniques to machine the substrate, usually silicon, and can be classified into isotropic and anisotropic techniques, or into wet and dry etching techniques. Wet etching is performed using liquid chemicals while dry etching is performed using gas-phase chemistry. Both methods can be either isotropic or anisotropic (Table 1). Isotropic etching provides the same etch rate in all directions whereas anisotropic etching provides different etch rates in different directions. Although wet etching is usually isotropic, the most common micromachining technique is the anisotropic wet etching of silicon in alkaline solution such as potassium hydroxide (KOH).

Table 1. Examples of etching techniques for machining the silicon substrate (Hierlemann *et al.*, 2003)

	Wet etching	Dry etching
Isotropic	HNA System – a mixture of hydrofluoric acid (HF), nitric acid (HNO ₃) and acetic acid (CH ₃ COOH)	Vapor phase etching: xenon difluoride (XeF ₂)
Anisotropic	Alkali Hydroxide Solutions: KOH, NaOH	Plasma etching Reactive Ion Etching (RIE) Deep RIE

The most common surface micromachining process is sacrificial-layer etching. In this process a microstructure is released by removing a sacrificial thin-film material, which was previously deposited underneath the microstructure.

3. TEMPERATURE MICRO-SENSOR

The micromechanical resonant sensor is an alternative to measure temperature with MEMS. The idea is to build a thermally excited micro-cantilever resonator, establishing a relationship between the first-order resonance and temperature. The analysis of frequency-temperature relation is essential for this kind of system being the objective of numerous articles, however, there are many effects that are not evaluated in literature.

The micro-resonator considered here was discussed by Han *et al.* (2002) and consists of a micro-cantilever beam shown in Figure 1. The original configuration, called *A*, has length $L = 1000\mu\text{m}$, width $200\mu\text{m}$ and thickness $h=11.2\mu\text{m}$. Different configurations are also treated in this work in order to evaluate the dimension influence in micro-scale: *B*, $1000\mu\text{m}$ length, $300\mu\text{m}$ width and $14.2\mu\text{m}$ thickness; *C*, $2000\mu\text{m}$ length, $200\mu\text{m}$ width and $15.8\mu\text{m}$ thickness. All configurations consider $1\mu\text{m}$ thickness for silicon layer. Excitation system of the micro-beam is based on piezoresistor set up. The micro-beam manufacturing considers lithography process together with boron diffusion and anisotropic etching of the substrate. The silicon layer is produced from oxidation of the upper part of the micro-resonator.

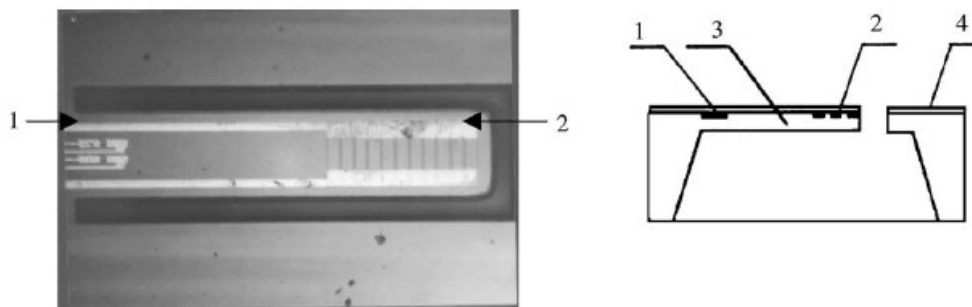


Figure 1. Microresonator beam (Han *et al.*, 2002):

1 –Wheatstone bridge, 2 – excitation resistor, 3 – silicon layer, 4 – silica layer.

There are many characteristics that can alter the system performance. Geometrical characteristics and dissipation are some of these aspects that should be taken into account in order to obtain accurate response of the sensor. In this regard, a finite element analysis is developed in order to verify the influence of dissipation on the temperature-frequency relation. Experimental data from Han *et al.* (2002) is used as reference for the verification of the finite element analysis. It is assumed that silicon has isotropic behavior.

Based on the analysis by Han *et al.* (2002), it is possible to verify some characteristics of the micro-resonator. Stemme (1991) proposes that the resonant frequency of a micro-beam is given by:

$$f_{10} = 0.162 \frac{h}{L^2} \sqrt{\frac{E}{\rho}} \quad (21)$$

where E is the Young modulus and ρ is the density.

By assuming a bi-layer micro-beam (Han *et al.*, 2002):

$$h = h_1 + h_2; \quad E = \frac{E_1 h_1 + E_2 h_2}{h_1 + h_2}; \quad \rho = \frac{\rho_1 h_1 + \rho_2 h_2}{h_1 + h_2}$$

Now, by considering that all parameters are temperature dependent, it is possible to write:

$$\begin{aligned} \kappa = \frac{1}{f_{10}} \frac{df_{10}}{dT} = & \frac{h_1}{2h_1 + 2h_2} \frac{1}{\frac{E_2}{E_1}} \frac{dE_1}{dT} + \frac{h_2}{2h_2 + 2h_1} \frac{1}{\frac{E_1}{E_2}} \frac{dE_2}{dT} \\ & - \frac{h_1}{2h_1 + 2h_2} \frac{1}{\frac{\rho_2}{\rho_1}} \frac{d\rho_1}{dT} - \frac{h_2}{2h_2 + 2h_1} \frac{1}{\frac{\rho_1}{\rho_2}} \frac{d\rho_2}{dT} + k_1 - k_2 \end{aligned}$$

where k is the linear expansion thermal coefficient. Therefore, the resonant frequency can be estimated as follows (Han *et al.*, 2002):

$$f_{10}(T) = f_{10}(T_0) [1 + \kappa(T - T_0)]$$

The analysis of the micro-scale behavior involving physical scaling laws, points that the air induces viscous damping to the micro-resonator beam. Han *et al.* (2002) establishes that this viscous damping has two components: dissipative component, proportional to velocity, and inertial component, proportional to acceleration. The combination of these two effects can be expressed by the following equation:

$$\gamma(T) = \frac{1}{2\rho h} \left(\frac{1}{12} \frac{PM}{RT} b + \frac{3}{4} \sqrt{\frac{PM\mu\pi}{RTf_1(T)}} \right)$$

where P is the air pressure, M is the air molecular mass, R is the air constant, μ is the air viscosity and b is the width of the micro-beam. Under this assumption, the frequency can be described by:

$$f_1(T) = f_1(T_0) [1 + \kappa(T - T_0) - \gamma(T) + \gamma(T_0)]$$

4. FINITE ELEMENT ANALYSIS

This contribution uses the finite element method (FEM) in order to model the micro-resonant beam. In brief, the FEM is employed to solve differential equations from splitting the domain in element where polynomial functions are used to approximate the solution. The general governing equation of the discrete system can be represented by:

$$[M]\{\ddot{U}\} + [C]\{\dot{U}\} + [K]\{U\} = \{F\}$$

where $[M]$ is the mass matrix, $[K]$ is the stiffness matrix, and $[C]$ is the damping matrix. In general, the damping matrix can be assumed to be proportional to stiffness and mass matrixes, being defined as follows:

$$[C] = \alpha[M] + \beta[K]$$

where α and β are real positive numbers. Note that the α parameter tends to influence low frequencies. The temperature dependence of FEM matrixes is defined from parameter variations. In this regard, the following expressions are employed to define the Young modulus, E , Poisson ratio, ν , and density, ρ , dependence using a reference temperature $T_0 = 298 \text{ K}$ (25°C).

$$E_i(T) = E_i(T_0) + E_i(T_0) \frac{1}{E_i} \frac{dE_i}{dT} (T - T_0)$$

$$\nu_i(T) = \nu_i(T_0) + \nu_i(T_0) \frac{1}{\nu_i} \frac{d\nu_i}{dT} (T - T_0)$$

$$\rho_i(T) = \rho_i(T_0) + \rho_i(T_0) \frac{1}{\rho_i} \frac{d\rho_i}{dT} (T - T_0)$$

Moreover, it is considered that the thermal expansion coefficient is constant. Table 2 presents silicon and silica properties (Han *et al.*, 2002; Kim, 1996; Gan *et al.*, 1996). Subscripts 1 refer to SiO_2 while 2 refer to Si.

Table 2. Materials properties used in the present model

$E_1(\text{GPa})$	67	$1/E_1(dE_1/dT) (\text{K}^{-1})$	192×10^{-6}
$E_2(\text{GPa})$	167	$1/E_2(dE_2/dT) (\text{K}^{-1})$	-52×10^{-6}
ν_1	0.17	$1/\nu_1(d\nu_1/dT) (\text{K}^{-1})$	0.75×10^{-6}
ν_2	0.278	$1/\nu_2(d\nu_2/dT) (\text{K}^{-1})$	-7.8×10^{-6}
$\rho_1(\text{Kg.m}^{-3})$	2200	$1/\rho_1(d\rho_1/dT) (\text{K}^{-1})$	-0.75×10^{-6}
$\rho_2(\text{Kg.m}^{-3})$	2330	$1/\rho_2(d\rho_2/dT) (\text{K}^{-1})$	-13×10^{-6}
$k_1(\text{K}^{-1})$	0.25×10^{-6}	$k_2(\text{K}^{-1})$	2.6×10^{-6}

Numerical simulations are performed using ABAQUS. Solid element C3D20, which is a second order cubic element with 20 nodes with 3 degrees of freedom each, is employed. Here, we are interested to establish the influence of damping in the frequency-temperature relation. Therefore, we define the critical damping coefficient (ABAQUS, 2006):

$$\xi = \frac{\alpha}{2\omega} + \frac{\beta\omega}{2}$$

and establishes an investigation considering different values of α and β , by evaluating different critical coefficient (1%, 2% and 5%, for example).

The finite element model of the micro-resonator beam is shown in Figure 2. The mesh is defined after a convergence analysis for each beam.

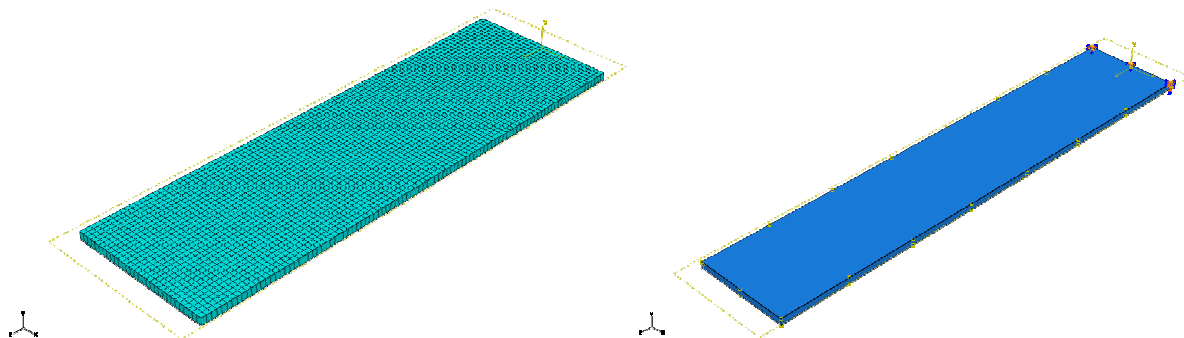


Figure 2. Finite element model of the micro-beam.

Initially, the micro-beam *A* is of concern (1000 μm length, 200 μm width and 11.2 μm thickness). Figure 3 presents the FEM simulations for different damping parameters together with experimental tests by Han *et al.* (2002). The increase of β parameter tends to move the simulation closer to experimental data and the value $\beta = 6.86 \times 10^{-6}\text{s}$ presents better results, representing a critical damping of 5.4%. Figure 3 also presents a comparison of the best FEM result with experimental data and the model proposed by Han *et al.* (2002). Note that the FEM model captures a linear variation.

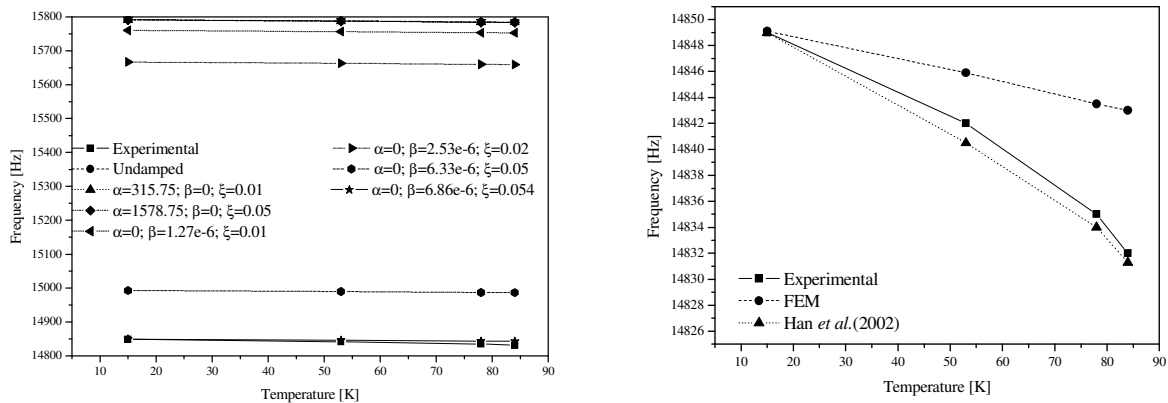


Figure 3. Micro-beam *A*: frequency-temperature relation.

The finite element analysis is now developed for micro-beam *B* (1000 μm length, 300 μm width and 14.2 μm thickness). Figure 4 presents the FEM simulations for different damping parameters together with experimental tests by Han *et al.* (2002). The same qualitative behavior is observed for this new configuration showing that the increase of β parameter tends to move the simulation closer to experimental data. Now, the value $\beta = 4.99 \times 10^{-6}\text{s}$ presents better results, representing a critical damping of 4.99%. Figure 4 also presents a comparison of the best FEM result with experimental data and the model proposed by Han *et al.* (2002).

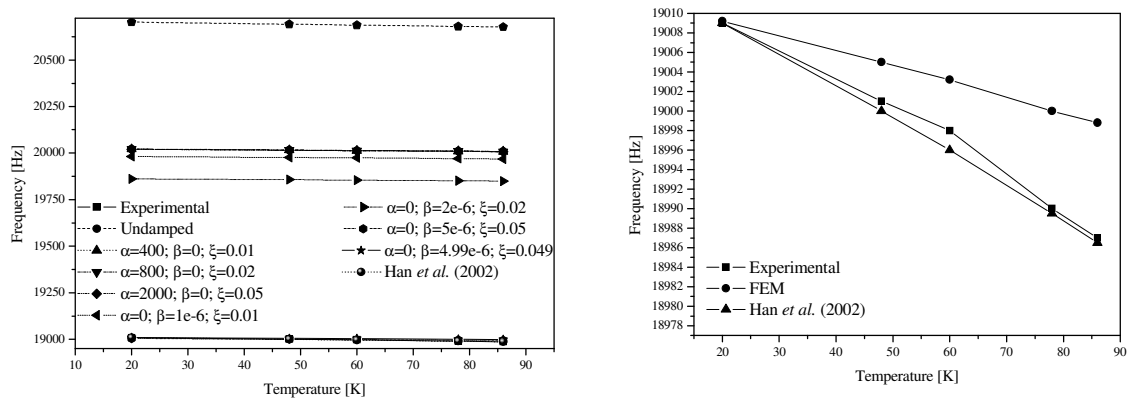


Figure 4. Micro-beam *B*: frequency-temperature relation.

A different configuration is now in focus. It is assumed micro-beam *C* has 2000 μm length, 200 μm width and 15.8 μm thickness. Once again, damping coefficients are modified in order to match experimental data. The general behavior of the other configurations is preserved and better results are obtained by increasing the parameter β . The best situation is obtained for $\beta = 1.546 \times 10^{-5}\text{s}$ that represents critical damping of 4.1%. Figure 5 presents the frequency-temperature curves for different damping coefficient and also establishes a comparison with experimental tests and results due to Han *et al.* (2002).

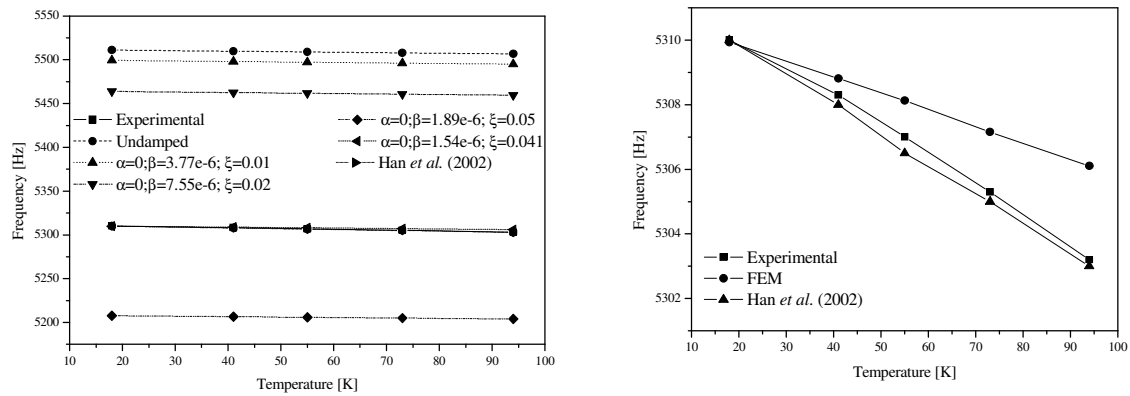


Figure 5. Micro-beam C: frequency-temperature relation.

The finite element analysis is interesting to evaluate different configurations confirming some behaviors. Here, the analysis of damping coefficients can be evaluated for different configurations of the micro-beam. Experimental data is adjusted by using a linear regression while model coefficients are evaluated from the first derivative of the temperature dependent curves. In order to present a systematic approach, it is defined an index that evaluate the FEM results with experimental data.

$$\Delta C_T = 100 \left[\frac{|C_T| - |C_T^{EXP}|}{|C_T^{EXP}|} \right]$$

Table 3. Temperature dependent coefficients.

Micro-beam	C_T^{FEM} [Hz.K ⁻¹]	C_T^{EXP} [Hz.K ⁻¹]	C_T^{Han} [Hz.K ⁻¹]	ΔC_T^{Han}	ΔC_T^{FEM}
A	-0.088±0.002	-0.24±0.03	-0.25±0.02	4 ± 8	63 ± 6
B	-0.159±0.003	-0.33±0.02	-0.340±0.007	3 ± 5	52 ± 4
C	-0.0507±0.0005	-0.090±0.003	-0.092±0.001	2 ± 1	44 ± 1

As expected from the analysis of physical law scaling, micro-beam with smaller dimensions tend to present a greater deviation of the temperature dependence coefficient that means that damping caused by the air increase in a proportional form as the dimension decreases.

5. CONCLUSIONS

This papers deals with a finite element analysis of micro-resonator used as temperature sensors. The main goal is to investigate the frequency-temperature relationship for different micro-beam configurations. Moreover, the influence of damping coefficient is of concern. The FEM analysis of the micro-beam establishes that smaller dimensions tend to present a greater deviation of the temperature dependence coefficient that means that damping caused by the air increase in a proportional form as the dimension decreases. This conclusion is in agreement with the physical law scaling, showing how the classical FEM can be applied to obtain important conclusions concerning MEMS.

6. ACKNOWLEDGEMENTS

The authors would like to acknowledge the support of the Brazilian Research Agency (CNPq) and the Rio de Janeiro's Research Agency (FAPERJ).

7. REFERENCES

- ABAQUS (2006), "Abaqus Theory Manual", D. Systèmes. Providence.
- Aravamudhan, S., Bhansali, S. (2008), "Reinforced piezoresistive pressure sensor for ocean depth measurements", *Sensors and Actuators A*, v.142, pp.111-117.
- Dubuc, D., Saddaoui, M., Melle, S., Flurens, F., Rabbia, L., et al. (2004), "Smart MEMS concept for high secure RF and millimeterwave communications", *Microelectronics Reliability*, v44, pp.899-907.
- Gan, L., B. Ben-Nissan, et al. (1996), "Modelling and finite element analysis of ultra-microhardness indentation of thin films", *Thin Solid Films*, v.290-291, pp.362-366.
- Gong S.-C. (2004), "Effects of pressure sensor dimensions on process window of membrane thickness", *Sensors and Actuators A*, v.112, pp. 286-290.
- Han, J., Zhu, C. et al. (2002), "Dependence of the resonance frequency of thermally excited microcantilever resonators on temperature", *Sensors and Actuators A*, v.101, n.1-2, pp.37-41.
- Hierlemann, A., Brand, O., Hagleitner, C. & Baltes, H. (2003), "Microfabrication Techniques for Chemical/Biosensors; *Proceedings of the IEEE*, v.91, n.6, pp.839-863.
- Judy, J. W. (2001), "Microelectromechanical systems (MEMS): Fabrication, design and applications", *Smart Materials and Structures*, v.10, n.6, p.1115-1134.
- Kaabi, L., Kaabi, A., Sakly, J. & AbdelMalek, F. (2007), "Modelling and analysis of MEMS sensor based on piezoresistive effects", *Materials Science and Engineering C*, v.27, pp.691-694.
- Kim, M. T. (1996), "Influence of substrates on the elastic reaction of films for the microindentation tests", *Thin Solid Films*, v.283, n.1-2, pp.12-16.
- Lin, L., Chu, H-C. & Lu, Y-W. (1999), "A simulation program for the sensitivity and linearity of piezoresistive pressure sensors", *Journal of Microelectromechanical Systems*, v.8, n.4, pp.514-522.
- Liu C. (2006), "*Foundations of MEMS*", Pearson Education.
- Madou, M. (1997), "*Fundamentals of microfabrication*". New York: CRC Press.
- Miyauchi, S., K. Kumagai, et al. (1991), "Microfabrication of diamond films: selective deposition and etching", *Surface & Coatings Technology*, v.47, n.1-3, p.465-473.
- Namazu, T., Hashizume, A. & Inoue, S. (2007), "Thermomechanical tensile characterization of Ti-Ni shape memory alloy films for design of MEMS actuators", *Sensors and Actuators A*, v.139, pp.178-186.
- Stemme, G. (1991), "Resonant silicon sensors", *Journal of Micromechanics and Microengineering*, v.1, n.2, p.113-125.
- Wang, C. & Madou, M. (2005), "From MEMS to NEMS with carbon", *Biosensors & Bioelectronics*, v.20, pp.2181-2187, 2005.
- Waterfall, T.L., Johns, G.K., Messenger, R.K., Jensen, B.D., McLain, T.W. & Howell L.L. (2008), "Observations of piezoresistivity for polysilicon in bending that are unexplained by linear models", *Sensors and Actuators A*, v.141, pp.610-618.

8. RESPONSIBILITY NOTICE

The authors are the only responsible for the printed material included in this paper.